taxane-based chemotherapy. We are even tempted to expect that the manipulative downregulation of SGOL1-B may increase the sensitivity of the cancer cells to taxane.

Methods

All experiments were performed in accordance with relevant guidelines and regulations. All the study protocols were approved by the Institutional Review Board of Hamamatsu University School of Medicine (reference number 23–91).

Tissue samples and nucleic acid extraction. Tissues from patients with primary NSCLC were surgically resected at the Hamamatsu University Hospital (Japan), Shimada Municipal Hospital (Japan), and Seirei Mikatahara General Hospital (Japan). Written informed consent was obtained from all subjects. Total RNA and genomic DNA were extracted from the tumors and normal tissues using the commercially available ISOGEN kit (Nippongene, Tokyo, Japan) and the DNeasy Tissue kit (QIAGEN, Valencia, CA, USA), according to the manufacturers' instructions. The tumor tissues were examined for somatic mutations in mutation cluster regions (hot spots) of the *EGFR* gene. The primers used for PCR and DNA sequencing have been described previously[39]. The study design was approved by the Institutional Review Boards of the relevant hospitals.

Quantitative real-time RT-PCR and plasmid construction. The structure and nomenclature of the transcripts of SGOL1 is shown in Figure 1a. Isoform SGOL1-B does not contain part of exon 6. We measured SGOL1-B, including both SGOL1-B1 and SGOL1-B2, using common primers. For the *in vitro* experiments, we used a construct of SGOL1-B1 containing exon 8.

Quantitative real-time RT-PCR was performed as described in our previous report[2]. The primer sequences used for the first RT-PCR for SGOL1 (Figure 1b) were as follows: forward, 5′-GACCCCAATAGTGATGACAGC-3′, reverse, 5′-GAAATGATTCTCCTTGTCCTGG-3′. For the amplification of each SGOL1 variant, the following primer sequences were used: the common forward primer for SGOL1-A, -B, and -C was 5′-CTCCAGAAATTTATTTGTGAAGG-3′, and the reverse primers for SGOL1-A, -B, and -C were 5′-CAAAATCAACTCCCAGTGT GTC-3′, 5′-GGTGGTGTAGCTGAATCAAAATC-3′, and 5′-GTTTCAGGTGG TGTAGCTTCTATTTG-3′, respectively. The *Glyceraldehyde-3-phosphate dehydrogenase* (*GAPDH*) transcript was amplified as an internal control, as described previously[2]. To express SGOL1-B1 in mammalian cells, three MYC tag sequences were fused to the 5′-side of SGOL1-B1 using PCR amplification, and the product was inserted into a pIRESpuro2 expression vector (Clontech, Palo Alto, CA, USA). A pSilencer plasmid with short hairpin RNA (shRNA) targeting the total SGOL1 and SGOL1-B sequences was used for the RNA interference (RNAi) procedure, as described previously[2]. The SGOL1-B shRNA expression vector was constructed by inserting shRNA sequences targeting SGOL1-B (target sequence: 5′-GATTCAGCT ACACCACCTGA-3′) into pSilencer 2.1-U6 puro (Applied Biosystems, Tokyo, Japan).

Fluorescence *in situ* hybridization (FISH) analysis. FISH analysis was performed on FFPE tumor samples and cell lines according to the manufacturers' instructions with minor modifications, as described previously[40,41]. Spectrum Orange-labeled BAC clones, RP11-106B16 (8p12, FGFR1), RP11-245 + RP11-355N16 (3q26.3, PIK3CA), RP11-275H4 (3q26.3, SOX2), RP11-51M22 (7q31.1, MET), and RP5-1091E12 (7q12, EGFR) (Advanced GenoTechs Co., Tsukuba, Japan), were used as locus-specific FISH probes. Spectrum Green-labeled control probes for the near centromere locus on chromosome 3 (RP11-91A15), 7 (RP11-90C3), and 8 (RP11-12L15) (Advanced GenoTechs Co.) were also used to enumerate the copies of chromosome 3, 7, and 8 in the FISH experiments. 4′,6-Diamidino-2-phenylindole (DAPI) (Vector Laboratories, Burlingame, CA, USA) was used for nuclear staining. At least 50 tumor cell nuclei were counted per case. Copy number amplification was defined by a BAC signal/CEP signal ratio greater than or equal to 2.0 or the presence of a tight gene cluster.

Cell culture and transfection. The human NSCLC cell lines A549 (adenocarcinoma), PC-3 (adenocarcinoma), H1299 (large cell carcinoma) and ACC-LC-176 (squamous cell carcinoma) were cultured at 37°C in RPMI medium (Invitrogen, Carlsbad, CA, USA) containing 5% or 10% fetal bovine serum (Nichirei, Tokyo, Japan) under 5% CO_2. The A549 and H1299 cell lines were gifts from Dr. Niki (Jichi Medical University), and the ACC-LC-176 cell line was a gift from Dr. Takahashi (Nagoya University). Transfection was performed using a Lipofectamine 2000 reagent (Invitrogen) according to the manufacturer's protocol.

Antibodies. Rabbit polyclonal anti-shugoshin (ab21633; Abcam, Cambridge, MA, USA) and anti-MYC tag (06-549; MILLIPORE, Bedford, MA, USA) antibodies and mouse monoclonal anti-β-tubulin (2-28-33; Sigma, St. Louis, MO, USA), anti-γ-tubulin (GTU88; Sigma), and anti-shugoshin (ab58023; Abcam) antibodies were used for western blotting and immunofluorescence staining as primary antibodies. A human autoantibody against the centromere (Immunovision, Springdale, AR, USA) was used for the immunofluorescent staining of the kinetochores. HRP-conjugated donkey polyclonal anti-rabbit antibody or anti-mouse IgG antibody (GE Healthcare, Piscataway, NJ, USA) and Alexa Fluor 488/546/633-conjugated goat polyclonal anti-rabbit, anti-mouse or anti-human IgG antibodies (Invitrogen) were used as secondary antibodies.

Western blotting. Cells were washed with PBS (–) and lysed with lysis buffer. The protein concentration of the lysate was measured using a BCA protein assay kit (Thermo Scientific, Rockford, IL, USA). Following the addition of sodium dodecyl sulfate (SDS) sample buffer, the samples were boiled, and ten micrograms of the cell lysate were subjected to SDS polyacrylamide gel electrophoresis. The electrophoresed proteins were then transferred to a membrane, and the protein of interest was detected using appropriate antibodies and the ECL Western Blotting Detection System (GE Healthcare), as described previously[42].

Indirect immunofluorescence analysis. Cells were washed with PBS and fixed with 4% paraformaldehyde at room temperature for 15 min or in methanol at −20°C for 5 min. After permeabilization and subsequent incubation with 10% normal goat serum blocking solution, the cells were probed with primary antibody. Indirect immunofluorescence labeling was then performed by exposure to Alexa Fluor-conjugated secondary antibody (Molecular Probes, Eugene, OR, USA), and the nuclei were stained with DAPI. The immunostained cells were examined under a confocal laser scanning microscope (FV1000; Olympus, Tokyo, Japan) or a fluorescence microscope (BZ-9000; KEYENCE, Osaka, Japan).

Chromosome spread. Transfected cells were selected with puromycin for 48 h and treated with 100 nM nocodazole (Sigma) for 20 h. They were then trypsinized and collected by centrifugation in a conical tube. The cells were gently suspended with hypotonic solution (75 mM KCl) and incubated at 37°C for 6 min. Chilled fixative solution (methanol/glacial acetic acid, 3 : 1) was gently added to the cells that had been collected by centrifugation, and this procedure consisting of centrifugation, cell collection, and the addition of chilled fixative solution was repeated three times. The fixed cells were dropped onto the slide glasses. After drying in air, they were stained with DAPI.

Time-lapse imaging. Cells were transfected with a total of 1 μg of expression vector for histone H2B-green fluorescent protein (GFP) together with an empty vector, the MYC-SGOL1-B1 expression vector, or the shRNA vector (molar ratio, 1 : 5). Docetaxel was then added to the growth medium of the control cells or the targeted shRNA-treated cells at 72 h after transfection (Figure 4c, 5b and 5e). After 48 h of culture, the medium was replaced with fresh medium and the cells were subjected to time-lapse imaging (FCV100; Olympus) using a device equipped with an incubation chamber. Fluorescence signals from the GFP were captured at 5-min intervals for 24 h, and the data were used to prepare a montage of images and movies. The image sequences were viewed using ImageJ software (version 1.43f; National Institutes of Health, Bethesda, MD, USA).

Growth inhibition assay. Cytotoxicity was evaluated using a WST-8 [2-(2-methoxy-4-nitrophenyl)-3-(4-nitrophenyl)-5-(2,4-disulphophenyl)-2H tetrazolium, monosodium salt] colorimetric assay. Cancer cells (5,000 cells/well) were seeded into 96-well cell plates in 100 μL of culture medium for 24 h before drug exposure. The cells were then treated with various concentrations of paclitaxel and docetaxel for 24 h. After drug exposure, the medium was discarded and replaced with 90 μL of fresh medium followed by the addition of 10 μL of WST-8 reagent solution (Cell Counting Kit; Dojindo Laboratories, Kumamoto, Japan) and incubated for 2 h at 37°C. Cell viability was determined by colorimetric comparison by reading the optical density values from a microplate reader at an absorption wavelength of 450 nm, according to the manufacturer's instructions.

Statistical analysis. The Mann-Whitney *U*-test was used to statistically analyze non-parametric data. The chi-square test or Fisher exact test was used to compare categorical variables. Differences in continuous variables were analyzed using the Student *t*-test for comparing 2 groups and using an ANOVA for multiple groups. Comparisons with $P < 0.05$ were considered statistically significant. The statistical analysis was performed using JMP software, version 7.0.1J (SAS Institute Japan, Tokyo, Japan).

1. Kitajima, T. S. *et al.* Shugoshin collaborates with protein phosphatase 2A to protect cohesin. *Nature* **441**, 46–52 (2006).
2. Iwaizumi, M. *et al.* Human Sgo1 downregulation leads to chromosomal instability in colorectal cancer. *Gut* **58**, 249–260 (2009).
3. Suzuki, H. *et al.* Human Shugoshin mediates kinetochore-driven formation of kinetochore microtubules. *Cell Cycle* **5**, 1094–1101 (2006).
4. Kahyo, T. *et al.* A novel tumor-derived SGOL1 variant causes abnormal mitosis and unstable chromatid cohesion. *Oncogene* **30**, 4453–4463 (2011).
5. Jemal, A., Siegel, R., Xu, J. & Ward, E. Cancer statistics. *CA Cancer J Clin.* **60**, 277–300 (2010).
6. Lynch, T. J. *et al.* Activating mutations in the epidermal growth factor receptor underlying responsiveness of non-small-cell lung cancer to gefitinib. *N Engl J Med* **350**, 2129–2139 (2004).
7. Soda, M. *et al.* Identification of the transforming EML4-ALK fusion gene in non-small-cell lung cancer. *Nature* **448**, 561–566 (2007).
8. Shinmura, K. *et al.* EML4-ALK fusion transcripts, but no NPM-, TPM3-, CLTC-, ATIC-, or TFG-ALK fusion transcripts, in non-small cell lung carcinomas. *Lung Cancer* **61**, 63–169 (2008).
9. Belani, C. P. *et al.* Randomized, phase III study of weekly paclitaxel in combination with carboplatin versus standard every-3-weeks administration of carboplatin

and paclitaxel for patients with previously untreated advanced non-small-cell lung cancer. *J Clin Oncol* **26**, 468–473 (2008).
10. Weaver, B. A. & Cleveland, D. W. Decoding the links between mitosis, cancer, and chemotherapy: The mitotic checkpoint, adaptation, and cell death. *Cancer Cell* **8**, 7–12 (2005).
11. Weiss, J. *et al.* Frequent and focal FGFR1 amplification associates with therapeutically tractable FGFR1 dependency in squamous cell lung cancer. *Sci Transl Med.* **2**, 62ra93 (2010).
12. Bass, A. J. *et al.* SOX2 is an amplified lineage-survival oncogene in lung and esophageal squamous cell carcinomas. *Nat Genet.* **41**, 1238–1242 (2009).
13. Okudela, K. *et al.* PIK3CA mutation and amplification in human lung cancer. *Pathol Int.* **57**, 664–671 (2007).
14. Cappuzzo, F. *et al.* Increased MET gene copy number negatively affects survival of surgically resected non-small-cell lung cancer patients. *J Clin Oncol.* **27**, 1667–1674 (2009).
15. Tsao, M. S. *et al.* Erlotinib in lung cancer - molecular and clinical predictors of outcome. *N Engl J Med.* **353**, 133–144 (2005).
16. Jordan, M. A. & Wilson, L. Microtubules and actin filaments: dynamic targets for cancer chemotherapy. *Curr Opin Cell Biol.* **10**, 123–130 (1998).
17. Gascoigne, K. E. & Taylor, S. S. Cancer cells display profound intra- and interline variation following prolonged exposure to antimitotic drugs. *Cancer Cell* **14**, 111–122 (2008).
18. Kitamura, S. *et al.* Peroxisome proliferator-activated receptor gamma induces growth arrest and differentiation markers of human colon cancer cells. *Jpn J Cancer Res.* **90**, 75–80 (1999).
19. Chang, T. H. & Szabo, E. Induction of differentiation and apoptosis by ligands of peroxisome proliferator-activated receptor γ in non-small cell lung cancer. *Cancer Res.* **60**, 1129–1138 (2000).
20. Passeron, T. *et al.* Upregulation of SOX9 inhibits the growth of human and mouse melanomas and restores their sensitivity to retinoic acid. *J Clin Invest.* **119**, 954–963 (2009).
21. Jiang, S. S. *et al.* Upregulation of SOX9 in lung adenocarcinoma and its involvement in the regulation of cell growth and tumorigenicity. *Clin Cancer Res.* **16**, 4363–4373 (2010).
22. Watanabe, Y., Ikemura, T. & Sugimura, H. Amplicons on human chromosome 11q are located in the early/late-switch regions of replication timing. *Genomics* **84**, 796–805 (2004).
23. Duijf, P. H. & Benezra, R. The cancer biology of whole-chromosome instability. *Oncogene* **32**, 1–10 (2013).
24. Dai, J., Kateneva, A. V. & Higgins, J. M. Studies of haspin-depleted cells reveal that spindle-pole integrity in mitosis requires chromosome cohesion. *J Cell Sci.* **122**, 4168–4176 (2009).
25. Shinmura, K. *et al.* Induction of centrosome amplification and chromosome instability in p53-deficient lung cancer cells exposed to benzo[a]pyrene diol epoxide (B[a]PDE). *J Pathol.* **216**, 365–374 (2008).
26. Xie, H. *et al.* Neoplastic transformation of human bronchial cells by lead chromate particles. *Am J Respir Cell Mol Biol.* **37**, 544–552 (2007).
27. Watanabe, Y. Shugoshin: guardian spirit at the centromere. *Curr Opin Cell Biol.* **17**, 590–595 (2005).
28. Ko, M. A. *et al.* Plk4 haploinsufficiency causes mitotic infidelity and carcinogenesis. *Nat Genet.* **37**, 883–888 (2005).
29. Aguirre-Portoles, C. *et al.* Tpx2 controls spindle integrity, genome stability, and tumor development. *Cancer Res.* **72**, 1518–1528 (2012).
30. Zelnak, A. B. Clinical pharmacology and use of microtubule-targeting agents in cancer therapy. *Methods Mol Med.* **137**, 209–234 (2007).
31. Yerushalmi, R., Woods, R., Ravdin, P. M., Hayes, M. M. & Gelmon, K. A. Ki67 in breast cancer: prognostic and predictive potential. *Lancet Oncol.* **11**, 174–183 (2010).
32. Honma, K. *et al.* RPN2 gene confers docetaxel resistance in breast cancer. *Nat Med.* **14**, 939–948 (2008).
33. Gan, P. P., Pasquier, E. & Kavallaris, M. Class III β-tubulin mediates sensitivity to chemotherapeutic drugs in non small cell lung cancer. *Cancer Res.* **67**, 9356–9363 (2007).
34. Seve, P. *et al.* Class III β -tubulin expression in tumor cells predicts response and outcome in patients with non-small cell lung cancer receiving paclitaxel. *Mol Cancer Ther.* **4**, 2001–2007 (2005).
35. Vilmar, A. C., Santoni-Rugiu, E. & Sorensen, J. B. Class III beta-tubulin in advanced NSCLC of adenocarcinoma subtype predicts superior outcome in a randomized trial. *Clin Cancer Res.* **17**, 5205–5214 (2011).
36. Janssen, A. & Medema, R. H. Mitosis as an anti-cancer target. *Oncogene* **30**, 2799–2809 (2011).
37. Milross, C. G. *et al.* Relationship of mitotic arrest and apoptosis to antitumor effect of paclitaxel. *J Natl Cancer Inst.* **88**, 1308–1314 (1996).
38. Torres, K. & Horwitz, S. B. Mechanisms of Taxol-induced cell death are concentration dependent. *Cancer Res.* **58**, 3620–3626 (1998).
39. Davies, H. *et al.* Somatic mutations of the protein kinase gene family in human lung cancer. *Cancer Res.* **65**, 7591–7595 (2005).
40. Sugimura, H. Detection of chromosome changes in pathology archives: an application of microwave-assisted fluorescence in situ hybridization to human carcinogenesis studies. *Carcinogenesis* **29**, 681–687 (2008).
41. Sugimura, H. *et al.* Fluorescence in situ hybridization analysis with a tissue microarray: 'FISH and chips' analysis of pathology archives. *Pathol Int.* **60**, 543–550 (2010).
42. Shinmura, K. *et al.* Reduced expression of MUTYH with suppressive activity against mutations caused by 8-hydroxyguanine is a novel predictor of a poor prognosis in human gastric cancer. *J Pathol.* **225**, 414–423 (2011).

Acknowledgments

We are grateful to Dr. Niki (Jichi Medical University, Shimotsuke, Japan) for providing us with a lung cancer cell line. We also acknowledge Mrs. K. Nagura, Mr. T. Kamo and Mr. S. Kageyama (Hamamatsu University School of Medicine) for their technical assistance. We appreciate Dr. Shuji Ogino (Brigham and Women's Hospital) and Dr. Mari Iida and Dr. Roger Wiseman (University of Wisconsin) for a critical reading of the manuscript. This work was supported by grants from the Ministry of Health, Labour and Welfare (19–19, 10103838), the Japan Society for the Promotion of Science (22590356, 23790396), Ministry of Education, Culture, Sports, Science and Technology (S-001), National Cancer Center Research and Development Fund, and the Smoking Research Foundation.

Author contributions

S.M. performed and designed the experiments, T.K., K.S., M.I. and H.Y. prepared the plasmid constructs, antibodies, and cells.K.F., J.K., M.T., H.N., H.O., N.I., T.S., H.S. and K.C. provided clinico-pathological data and analyses. T.K., K.S., M.I., T.T. and Y.W. input the discussion and arguments from the standpoint of cell biology. S.M., T.K., K.S., and H.S. wrote the manuscript. H.S. conceived the whole plan integrating clinicals, FISH analyses, and in vitro scheme. All the authors reviewed the manuscript.

Additional information

Supplementary information accompanies this paper at http://www.nature.com/scientificreports

Competing financial interests: The authors declare no competing financial interests.

How to cite this article: Matsuura, S. *et al.* SGOL1 variant B induces abnormal mitosis and resistance to taxane in non-small cell lung cancers. *Sci. Rep.* 3, 3012; DOI:10.1038/srep03012 (2013).

A novel somatic *FGFR3* mutation in primary lung cancer

KAZUYA SHINMURA[1], HISAMI KATO[1], SHUN MATSUURA[1,2], YUSUKE INOUE[1,2], HISAKI IGARASHI[1], KIYOKO NAGURA[1], SATOKI NAKAMURA[1], KYOKO MARUYAMA[1], MARI TAJIMA[1], KAZUHITO FUNAI[3], HIROSHI OGAWA[4], MASAYUKI TANAHASHI[5], HIROSHI NIWA[5] and HARUHIKO SUGIMURA[1]

Departments of [1]Tumor Pathology, [2]Internal Medicine 2 and [3]Surgery 1, Hamamatsu University School of Medicine, Hamamatsu, Shizuoka 431-3192; Divisions of [4]Pathology and [5]Thoracic Surgery, Respiratory Disease Center, Seirei Mikatahara General Hospital, Hamamatsu, Shizuoka 433-8558, Japan

Received October 9, 2013; Accepted November 25, 2013

DOI: 10.3892/or.2014.2984

Abstract. The recent discovery of mutations and fusions of oncokinase genes in a subset of lung cancers (LCs) is of considerable clinical interest, since LCs containing such mutations or fusion transcripts are reportedly sensitive to kinase inhibitors. To better understand the role of the recently identified fibroblast growth factor receptor 3 (*FGFR3*) mutations and fusions in pulmonary carcinogenesis, we examined 214 LCs for mutations in the mutation cluster region of the *FGFR3* gene using sequencing analysis. We also examined 190 LCs for the FGFR3-TACC3 and FGFR3-BAIAP2L1 fusion transcripts using reverse transcription-polymerase chain reaction (RT-PCR) analysis. Although the expression of FGFR3-TACC3 and FGFR3-BAIAP2L1 fusion transcripts was not detected in any of the carcinomas, somatic *FGFR3* mutations were detected in two (0.9%) LCs. The two mutations were the same, i.e., p.R248H. That was a novel mutation occurring in the same codon as p.R248C, for which an oncogenic potential has previously been shown. Increased FGFR3 expression was shown in the two LCs containing the *FGFR3* p.R248H mutation using qPCR. Histologically, both carcinomas were squamous cell carcinomas, therefore the incidence of the *FGFR3* mutation among the squamous cell carcinoma cases was calculated as 3.2% (2/63). When we examined other co-occurring genetic abnormalities, one case exhibited a *p53* p.R273C mutation, while the other case exhibited *PIK3CA* and *SOX2* amplifications. The above results suggest that an *FGFR3* p.R248H mutation is involved in the carcinogenesis of a subset of LCs and may contribute to the elucidation of the characteristics of *FGFR3* mutation-positive LCs in the future.

Correspondence to: Dr Kazuya Shinmura, Department of Tumor Pathology, Hamamatsu University School of Medicine, 1-20-1 Handayama, Higashi Ward, Hamamatsu, Shizuoka 431-3192, Japan
E-mail: kzshinmu@hama-med.ac.jp

Key words: fibroblast growth factor receptor 3, somatic mutation, fusion gene, lung cancer, squamous cell carcinoma

Introduction

Mutations of *EGFR*, *KRAS*, *PIK3CA*, and others, and fusion transcripts of ALK, ROS1 and RET are oncogenic alterations in lung cancers (LCs) and some of them are therapeutic targets (1-8). For example, crizotinib, a small molecule inhibitor of ALK, has been shown to selectively inhibit the growth of ALK-positive LC (9), meaning that a subclass of LC patients are likely to benefit clinically from an ALK inhibitor. Therefore, targetable oncogenic alterations in LCs may have a significant clinical impact.

Fibroblast growth factor receptor 3 (FGFR3) has been revealed to be activated by the mutation or fusion of its own gene in several types of cancer, such as urinary bladder cancer, glioblastoma, rhabdomyosarcoma and LC (10-17). Some tumor-specific *FGFR3* mutations, including p.R248C and p.S249C, drive the anchorage-independent growth of NIH3T3 cells and tumor formation in xenograft models, and cells harboring such *FGFR3* mutations showed an enhanced sensitivity to BGJ398, a selective FGFR kinase inhibitor (17). Regarding fusions, FGFR3-TACC3 and FGFR3-BAIAP2L1 oncogenic fusions have thus far been identified (13-15), and cells harboring the FGFR3-TACC3 fusion showed enhanced sensitivity to three FGFR kinase inhibitors, including BGJ398 (13). Thus, oncogenic *FGFR3* mutations and fusions in tumors can be therapeutic targets. To determine which patients can benefit from FGFR inhibitors in the future, the incidence of *FGFR3* mutations or fusions in various tumors derived from patients from various demographic areas must be determined. However, to date, only a few studies have been published regarding *FGFR3* mutations and fusions in LC and Asian patients with LC have not yet been analyzed (12,16,17). Notably, according to previous reports (12,16,17), the only experimentally proven oncogenic *FGFR3* mutations in LCs are p.R248C and p.S249C, which are located within the first ten bases of exon 7. Therefore, we considered this region to be a mutation cluster region in LCs. In the present study, to determine the status of *FGFR3* mutation and fusion in LCs derived from Japanese patients, we examined LCs from Japanese patients for the mutations in the mutation cluster region of *FGFR3* and the expression of FGFR3-TACC3 and FGFR3-BAIAP2L1 fusion transcripts and pathologically and molecularly characterized LCs containing such an alteration.

This is the first published study to describe *FGFR3* mutations in LCs derived from Japanese patients.

Materials and methods

Primary LC. Samples of surgical specimens were obtained from 362 Japanese LC patients who underwent surgery for cancer at Hamamatsu University Hospital and Mikatahara Seirei General Hospital. Informed consent was obtained from all the patients, and the study was approved by the Institutional Review Boards (IRBs) of Hamamatsu University School of Medicine and Mikatahara Seirei General Hospital. The clinicopathological profiles of the cases are shown in Table I. The histological classification was based on the World Health Organization system. Among the 362 cases, 214 cases were used in the mutational analysis, whereas 190 cases were used in the reverse transcription-polymerase chain reaction (RT-PCR) analysis; 42 cases were used in both analyses.

Search for FGFR3 mutations using PCR-sequencing. Genomic DNAs were extracted from the lung tissue samples using a DNeasy kit (Qiagen, Valencia, CA, USA) and were examined for somatic mutations in the DNA sequences (the first half of exon 7) covering the mutation cluster region in the *FGFR3* gene. PCR was performed in 20-μl reaction mixtures containing HotStarTaq DNA polymerase (Qiagen) under the following conditions: 30 sec at 94°C, 30 sec at 65°C and 60 sec at 72°C for 45 cycles. The following set of primers was used: 5'-CTG AGC GTC ATC TGC CCC C-3' and 5'-TGG GGC TGT GCG TCA CTG TAC-3'. PCR-amplified products were purified with ExoSAP-IT (GE Healthcare Bio-Sciences, Piscataway, NJ, USA) and were sequenced directly using a BigDye Terminator Cycle Sequencing Reaction kit (Applied Biosystems, Tokyo, Japan) and the ABI 3130 Genetic Analyzer (Applied Biosystems).

Search for FGFR3 fusion transcripts using RT-PCR. Total RNA was extracted from the lung tissue samples using an RNeasy kit (Qiagen) and was converted to first-strand cDNA using a SuperScript First-Strand Synthesis System for RT-PCR (Invitrogen, Carlsbad, CA, USA) according to the supplier's protocol. PCR was performed in 20-μl reaction mixtures containing HotStarTaq DNA polymerase under the following conditions: 30 sec at 94°C, 30 sec at 59°C and 60 sec at 72°C for 45 cycles. The following reverse PCR primers were used: 5'-CAG CCT CCA CTG GTT TCT GTA G-3' for the sequence at exon 4 of TACC3, 5'-TGG TAC ACA ACC TCT TCG AAC C-3' for the sequence at exon 12 of TACC3, and 5'-GGA CAT GTC CCA GTT CAG TTG-3' for the sequence at exons 3 and 4 of BAIAP2L1. The forward PCR primer used was the same, i.e., 5'-GAC CGT GTC CTT ACC GTG AC-3' for the sequence at exon 18 of FGFR3. The PCR products were fractionated using electrophoresis on an agarose gel and were stained with ethidium bromide.

Quantitative RT (qRT)-PCR. The expressions of the FGFR3 mRNA transcripts were measured using real-time qRT-PCR with a LightCycler instrument (Roche, Palo Alto, CA, USA). PCR amplification of the FGFR3 transcript and the transcript of the control housekeeping gene *GAPDH* was performed with the cDNA and a QuantiTect SYBR Green PCR kit (Qiagen). The following PCR primers were used: 5'-GCA CAC ACG ACC TGT ACA TGA TC-3' and 5'-CCA GGT ACT CGT CGG TGG AC-3' for the FGFR3 transcript, and 5'-GCT CAG ACA CCA TGG GGA AG-3' and 5'-TGT AGT TGA GGT CAA TGA AGG GG-3' for the GAPDH transcript. The T/N ratios were calculated by dividing the normalized transcript amounts in the cancerous tissue by the amounts in the non-cancerous tissue.

Table I. Summary of the clinicopathological profiles of the patients.

Characteristics	Number[a]		
	Total	Mutational analysis	RT-PCR analysis
No. of patients	362	214	190
Age, years (mean ± SD)	66.5±9.6	66.4±9.7	66.9±9.9
Gender, n (%)			
Male	259 (71.5)	157 (73.4)	134 (70.5)
Female	103 (28.5)	57 (26.6)	56 (29.5)
Histology, n (%)			
Adenocarcinoma	210 (58.0)	125 (58.4)	109 (57.4)
Squamous cell carcinoma	110 (30.4)	63 (29.4)	60 (31.6)
Large cell carcinoma	13 (3.6)	9 (4.2)	5 (2.6)
Small cell carcinoma	12 (3.3)	11 (5.1)	3 (1.6)
Adenosquamous carcinoma	11 (3.0)	4 (1.9)	9 (4.7)
Pleomorphic carcinoma	6 (1.7)	2 (0.9)	4 (2.1)

[a]Forty-two cases were used in both the mutational analysis and the RT-PCR analysis. SD, standard deviation. RT-PCR, reverse transcription-polymerase chain reaction.

Immunohistochemical staining. Sections of formalin-fixed, paraffin-embedded tissue samples were used for immunohistochemical staining using a Histofine Simple Stain MAX PO kit (Nichirei, Tokyo, Japan), as previously described (18). The primary antibodies were: anti-CK14, anti-thyroid transcription factor-1 (TTF-1) (both from Novocastra Laboratories, Newcastle, UK) and anti-p53 (clone DO7; Dako, Tokyo, Japan). Hematoxylin and eosin (H&E) staining was also performed.

Search for EGFR, KRAS, PIK3CA and p53 mutations using PCR-sequencing. Genomic DNA derived from the lung tissue samples containing an *FGFR3* mutation was examined for somatic mutations in the DNA sequences of mutation cluster regions in the *EGFR*, *KRAS*, *PIK3CA* and *p53* genes. PCR amplification was performed as previously described (7). Sequencing was performed as described in the 'Search for *FGFR3* mutations using PCR-sequencing' section.

Fluorescence in situ hybridization (FISH) analysis. Paraffin-embedded tissue sections were de-waxed and re-hydrated, then

boiled in 0.01 M citrate buffer (pH 6.0) to release the closed chromosomal structures. A combination of Cy3-labeled bacterial artificial chromosome (BAC) clone (RP11-100B16) for the *FGFR1* locus, BAC clone (RP11-245C23 and RP11-355N16) for the *PIK3CA* locus, or BAC clone (RP11-275H4) for the *SOX2* locus and a SpectrumGreen-labeled control BAC probe for the near centromere locus on chromosome 3 or 8 were placed on a slide and covered with a coverslip. All the BAC probes were obtained from Advanced GenoTechs Co. (Tsukuba, Japan). The slides with the hybridization mixture were denatured on a digital hot plate (HP-15; As One Corporation, Osaka, Japan) and then incubated overnight at 42°C. After washing the slide in 50% formamide/2X SSC, mounting medium containing DAPI (Vector Laboratories, Burlingame, CA, USA) was used for nuclear counterstaining. The slides were promptly examined under a fluorescence microscope (Olympus BX51-FL; Olympus, Tokyo, Japan) equipped with epifluorescence filters and a photometric CCD camera (Sensicam; PCO Company, Kelheim, Germany). The images captured were digitized and stored in the image analysis program (MetaMorph; Molecular Devices, Palo Alto, CA, USA). The average ratio of the *FGFR1*, *PIK3CA*, or *SOX2* signal number to the control probe signal number was calculated for each cancer. If the ratio of a cancer was >2.5, the cancer was defined as amplification-positive.

Results

In the present study, we examined 214 LCs for mutations in the mutation cluster region of the *FGFR3* gene using a sequencing analysis; we also examined 190 LCs for FGFR3-TACC3 and FGFR3-BAIAP2L1 fusion transcripts using an RT-PCR analysis. Although the expression of FGFR3-TACC3 and FGFR3-BAIAP2L1 fusion transcripts was not detected in any of the carcinomas, *FGFR3* mutations were detected in two (0.9%) LCs (Fig. 1A). The mutations that occurred in the LCs derived from cases no. 57 and no. 183 were the same, i.e., a somatic c.743G>A mutation associated with an amino acid exchange from Arg to His at codon 248. The p.R248H mutation in the *FGFR3* gene has not been previously reported, suggesting it is a novel mutation. Of note, with regards to codon 248, it was previously reported that the p.R248C mutation drives cellular transformation (17), indicating that the p.R248H mutation may have an oncogenic potential similar to that of the p.R248C mutation. When we next examined the expression levels of FGFR3 mRNA transcripts in the two LCs containing an *FGFR3* p.R248H mutation using a qRT-PCR analysis, the ratio of the level of FGFR3 mRNA expression in the cancerous tissue to the level in the corresponding non-cancerous tissue (T/N ratio) was increased in both cases (Fig. 1B), suggesting the involvement of mutated FGFR3 in LC. Case no. 57 was a 62-year-old man who was a smoker [Brinkman index (BI)=1,800] and case no. 183 was a 66-year-old man who was also a smoker (BI=1,000). The histological classification of both LCs was squamous cell carcinoma (Fig. 2A and B). An immunohistochemical study revealed that the carcinomas were positive for CK14 but negative for TTF-1 (Fig. 2C and D, Table II), indicating that the immunophenotype of the carcinoma was compatible with that of squamous cell carcinoma. Among the 214 cases used for the mutational analysis, 63 cases were histologically classified as

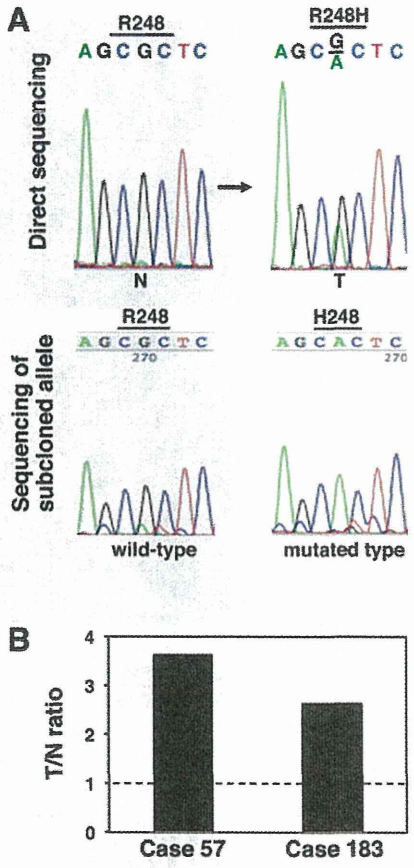

Figure 1. Detection of *FGFR3* mutations in primary lung cancer (LC). (A) Results of direct sequencing analysis of the *FGFR3* gene in LC DNA derived from case no. 183 (upper panels) and results of sequencing analysis of the subcloned PCR product covering the mutation in the case (lower panels). A somatic CGC to CAC mutation associated with the conversion from Arg to His at codon 248 was detected in the LC. N, non-cancerous lung tissue DNA; T, cancerous lung tissue DNA. In the analysis of subcloned products, both wild-type and mutated-type alleles were detected. (B) Comparison between FGFR3 mRNA expression in cancerous tissues from two LCs containing an *FGFR3* mutation and corresponding non-cancerous lung tissues, as determined using a qRT-PCR analysis. After normalizing the amounts of FGFR3 transcripts to those of the GAPDH transcripts, the T/N values were calculated by dividing the amount of normalized transcripts in the cancerous tissue by the amount in the corresponding non-cancerous tissue. FGFR3, fibroblast growth factor receptor 3.

squamous cell carcinoma; thus, the incidence of the *FGFR3* mutation among the squamous cell carcinoma cases was 3.2% (2/63). These findings suggest that a subset of LC may carry an *FGFR3* mutation.

We next examined whether the LC cases containing the *FGFR3* p.R248H mutation also contained mutations in other genes that are often mutated in LC (3,8,12,19,20). Mutation cluster regions for *EGFR*, *KRAS*, *PIK3CA* and *p53* (3,8,12,19,20) were searched for somatic mutations. No somatic mutations in exon 2 of *KRAS*, exons 19 and 21 of *EGFR*, or exons 9 and 20 of *PIK3CA* were detected; however, a somatic c.817C>T mutation associated with an amino acid exchange from Arg to Cys at codon 273 (p.R273C) was detected in the *p53* gene in case no. 183 (Fig. 2E, Table II). The fact that the missense mutation was detected in the DNA binding region of the p53 protein suggested that the mutant p53 protein was stable in the cancer

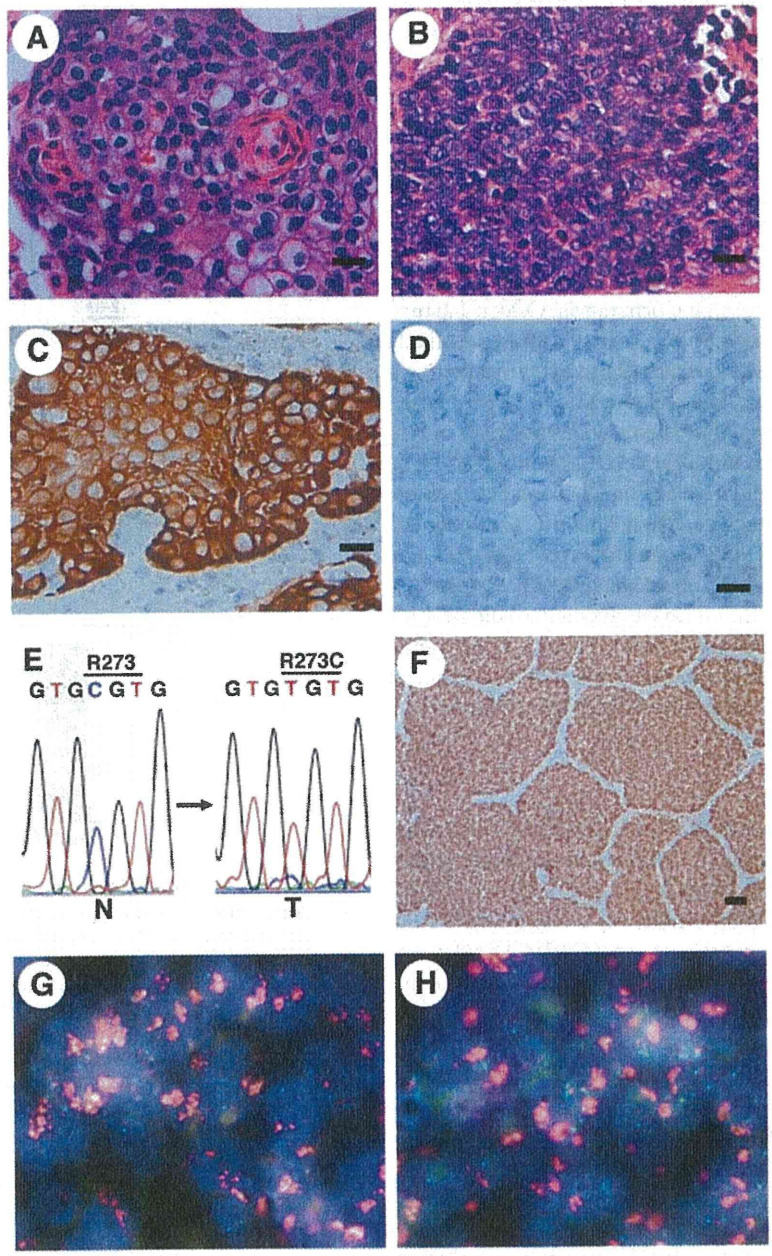

Figure 2. Pathological, immunohistochemical, mutational and FISH analyses for lung cancers (LCs) containing an *FGFR3* mutation. (A and B) Microscopic image (H&E) of the squamous cell carcinoma in case no. 57 (A) and case no. 183 (B). Scale bar, 20 μm. (C and D) The squamous cell carcinoma of case no. 57 was immunohistochemically positive for CK14 (C) and negative for TTF-1 (D). Scale bar, 20 μm. (E) Detection of a somatic *p53* missense mutation in LC from case no. 183. A CGT to TGT mutation associated with the conversion from Arg to Cys at codon 273 was detected in the LC. N, non-cancerous lung tissue DNA; T, cancerous lung tissue DNA. (F) Immunohistochemical detection of p53 accumulation in the LC from case no. 183. Scale bar, 50 μm. (G and H) *PIK3CA* (G) and *SOX2* (H) amplifications in LC from case no. 57, as shown using a FISH analysis. Red signals, BAC probe for the *PIK3CA* (G) and *SOX2* (H) locus; green signals, control probe for the near centromere locus on chromosome 3. FGFR3, fibroblast growth factor receptor 3; H&E, hematoxylin and eosin; TTF-1, thyroid transcription factor-1.

cells. We therefore performed immunohistochemical staining for p53 in case no. 183 and the results showed the nuclear accumulation of p53 exclusively in the cancer cells (Fig. 2F). These results suggested that a somatic *p53* mutation, but not *EGFR*, *KRAS* or *PIK3CA* mutations, may occur in a subset of LCs containing an *FGFR3* mutation.

We also examined whether the LC cases containing the *FGFR3* p.R248H mutation also contained gene amplifications, which are frequently observed in LC (12,21,22). The amplification status of the *FGFR1*, *PIK3CA* and *SOX2* genes was examined using a FISH analysis. Although *FGFR1* amplification was not detected in either case, the amplification of the *PIK3CA* and *SOX2* genes was detected in case no. 57 (Fig. 2G and H, Table II). These results suggested that *PIK3CA* and *SOX2* gene amplification, but not *FGFR1*, may occur in a subset of LCs containing an *FGFR3* mutation.

Table II. Clinical profiles of the cases with LC containing an *FGFR3* mutation and the pathological, immunohistochemical, mutational and amplification status of the LCs.

Characteristics	Case No. 57	Case No. 183
FGFR3 mutation	p.R248H	p.R248H
Age (years)	62	66
Gender	Male	Male
Smoking habit	Smoker (BI=1,800)	Smoker (BI=1,000)
Histology	Squamous cell carcinoma	Squamous cell carcinoma
Stage	III	II
Lymph node metastasis	Positive	Positive
CK14 expression	Positive	Positive
TTF-1 expression	Negative	Negative
EGFR mutation (exons 19 and 21)	Wild-type	Wild-type
KRAS mutation (exon 2)	Wild-type	Wild-type
PIK3CA mutation (exons 9 and 20)	Wild-type	Wild-type
p53 mutation (exons 4-9)	Wild-type	p.R273C mutation
FGFR1 amplification	Amplification (-)	Amplification (-)
PIK3CA amplification	Amplification (+)	Amplification (-)
SOX2 amplification	Amplification (+)	Amplification (-)

BI, Brinkman index; LC, lung cancer; FGFR3, fibroblast growth factor receptor 3;TTF-1, thyroid transcription factor-1.

Discussion

In the present study, *FGFR3* mutations were found in two (0.9%) of the 214 LCs that were examined, but the expression of FGFR3-TACC3 and FGFR3-BAIAP2L1 fusion transcripts was not detected in any of the 190 LCs that were examined. Both LCs containing an *FGFR3* mutation were histologically diagnosed as squamous cell carcinoma, and squamous cell carcinoma accounted for 63 out of the 214 LCs examined in the mutational analysis, resulting in an incidence of *FGFR3* mutation among squamous cell carcinoma cases of 3.2% (2/63). Both of the mutations were p.R248H, which was a novel mutation located in the same codon as the oncogenic p.R248C mutation. Both LCs exhibited an increased FGFR3 expression, suggesting the involvement of mutated FGFR3 in LC. Regarding the co-occurring genetic abnormalities, one case exhibited a *p53* p.R273C mutation, while the other case exhibited *PIK3CA* and *SOX2* amplifications. No somatic mutations were detected in the mutation cluster regions of the *EGFR*, *KRAS* and *PIK3CA* genes in either case. These results suggested that an *FGFR3* p.R248H mutation is involved in the carcinogenesis of a subset of LCs.

A novel p.R248H mutation in the *FGFR3* gene was detected in two lung squamous cell carcinomas derived from Japanese patients with a smoking habit. The detection of the p.R248H mutation in two LCs suggests a recurrent mutation in LC. The p.R248C mutation occurred in the same codon as the p.R248H mutation and was previously shown to drive cellular transformation; additionally, the transformation was shown to be reversed by a small molecule FGFR inhibitor (17). Moreover, the p.R248C mutation was detected not only in LC, but also in urinary bladder cancer and multiple myeloma (10,11,23). Regarding the amino acid conversion from Arg to His, p.R175H and p.R273H in the *p53* gene are hotspot mutations and gain-of-function mutations (24,25), suggesting the effect of the amino acid exchange on carcinogenesis. In addition, the screening for non-acceptable polymorphisms (SNAP) program, which predicts the effect of single amino acid substitutions on protein function (http://www.rostlab.org/services/SNAP) (26), predicted that the *FGFR3* p.R248H mutation was non-neutral. Finally, in our qRT-PCR experiment, an increased FGFR3 expression was detected in both LCs containing a p.R248H mutation. Thus, the *FGFR3* p.R248H mutation may play an important role in the genesis and development of LCs. In the future, a precise functional investigation may aid in clarifying the role of the *FGFR3* p.R248H mutation.

There have been two previous reports investigating *FGFR3* mutations. Activating *FGFR3* mutations were detected at a frequency of 2.2% (4/178 squamous cell carcinomas) in one study (12) and 4.2% (2/48 squamous cell carcinomas) in another report (16). In the present study, the incidence of *FGFR3* mutation among squamous cell carcinomas derived from Japanese patients was 3.2%, although functional characterization of the mutant was not performed. These results suggested that *FGFR3* mutation is a recurrent event in lung squamous cell carcinomas in multiple populations.

FGFR3 fusion transcripts were previously found in one study at a frequency of 4.2% (2/48 squamous cell carcinomas) (16). On the other hand, no FGFR3 fusion transcripts were detected in our cases, suggesting that FGFR3 fusion may be rare in the Japanese population. However, since the number of analyzed squamous cell carcinoma cases in our study was relatively small (n=60) and FGFR3 may be fused with proteins other than TACC3 and BAIAP2L1, a future large study examining this issue is required to examine the incidence of FGFR3 fusion in LCs derived from Japanese patients.

In our *FGFR3* mutation-positive cases, the co-occurrence of *p53* mutation in one case and the co-occurrence of *PIK3CA* and *SOX2* amplification in the other case were observed. Both *p53* mutation and amplification of the *PIK3CA* and *SOX2* genes are frequent in lung squamous cell carcinoma (12,21,22). These results suggest that a combination of *FGFR3* mutation and such alterations may favor lung squamous cell carcinoma and *FGFR3* mutation is not mutually exclusive with such alterations in lung squamous cell carcinoma.

In conclusion, our *FGFR3* mutation-positive LCs in conjunction with previously detected *FGFR3* mutation-positive LCs suggested that an *FGFR3* mutation is involved in the carcinogenesis of a subset of LCs, especially lung squamous cell carcinomas, and may aid in elucidating the characteristics of *FGFR3* mutation-positive LCs in the future.

Acknowledgements

The authors wish to acknowledge Mr. T. Kamo (Hamamatsu University School of Medicine) for his technical assistance. The present study was supported in part by a grant-in-aid from the Ministry of Health, Labour and Welfare (21-1), a grant-in-aid from the Japan Society for the Promotion of Science (25460476), a grant-in-aid from the Ministry of Education, Culture, Sports, Science and Technology (221S0001), and the Smoking Research Foundation.

References

1. Soda M, Choi YL, Enomoto M, Takada S, Yamashita Y, Ishikawa S, Fujiwara S, Watanabe H, Kurashina K, Hatanaka H, Bando M, Ohno S, Ishikawa Y, Aburatani H, Niki T, Sohara Y, Sugiyama Y and Mano H: Identification of the transforming *EML4-ALK* fusion gene in non-small-cell lung cancer. Nature 448: 561-566, 2007.
2. Shinmura K, Kageyama S, Tao H, Bunai T, Suzuki M, Kamo T, Takamochi K, Suzuki K, Tanahashi M, Niwa H, Ogawa H and Sugimura H: EML4-ALK fusion transcripts, but no NPM-, TPM3-, CLTC-, ATIC-, or TFG-ALK fusion transcripts, in non-small cell lung carcinomas. Lung Cancer 61: 163-169, 2008.
3. Schmid K, Oehl N, Wrba F, Pirker R, Pirker C and Filipits M: *EGFR/KRAS/BRAF* mutations in primary lung adenocarcinomas and corresponding locoregional lymph node metastases. Clin Cancer Res 15: 4554-4560, 2009.
4. Kohno T, Ichikawa H, Totoki Y, Yasuda K, Hiramoto M, Nammo T, Sakamoto H, Tsuta K, Furuta K, Shimada Y, Iwakawa R, Ogiwara H, Oike T, Enari M, Schetter AJ, Okayama H, Haugen A, Skaug V, Chiku S, Yamanaka I, Arai Y, Watanabe S, Sekine I, Ogawa S, Harris CC, Tsuda H, Yoshida T, Yokota J and Shibata T: *KIF5B-RET* fusions in lung adenocarcinoma. Nat Med 18: 375-377, 2012.
5. Takeuchi K, Soda M, Togashi Y, Suzuki R, Sakata S, Hatano S, Asaka R, Hamanaka W, Ninomiya H, Uehara H, Lim Choi Y, Satoh Y, Okumura S, Nakagawa K, Mano H and Ishikawa Y: RET, ROS1 and ALK fusions in lung cancer. Nat Med 18: 378-381, 2012.
6. Lipson D, Capelletti M, Yelensky R, Otto G, Parker A, Jarosz M, Curran JA, Balasubramanian S, Bloom T, Brennan KW, Donahue A, Downing SR, Frampton GM, Garcia L, Juhn F, Mitchell KC, White E, White J, Zwirko Z, Peretz T, Nechushtan H, Soussan-Gutman L, Kim J, Sasaki H, Kim HR, Park SI, Ercan D, Sheehan CE, Ross JS, Cronin MT, Jänne PA and Stephens PJ: Identification of new *ALK* and *RET* gene fusions from colorectal and lung cancer biopsies. Nat Med 18: 382-384, 2012.
7. Matsuura S, Shinmura K, Kamo T, Igarashi H, Maruyama K, Tajima M, Ogawa H, Tanahashi M, Niwa H, Funai K, Kohno T, Suda T and Sugimura H: CD74-ROS1 fusion transcripts in resected non-small cell lung carcinoma. Oncol Rep 30: 1675-1680, 2013.
8. Oxnard GR, Binder A and Jänne PA: New targetable oncogenes in non-small-cell lung cancer. J Clin Oncol 31: 1097-1104, 2013.
9. Casaluce F, Sgambato A, Maione P, Rossi A, Ferrara C, Napolitano A, Palazzolo G, Ciardiello F and Gridelli C: ALK inhibitors: a new targeted therapy in the treatment of advanced NSCLC. Target Oncol 8: 55-67, 2013.
10. Cappellen D, De Oliveira C, Ricol D, de Medina S, Bourdin J, Sastre-Garau X, Chopin D, Thiery JP and Radvanyi F: Frequent activating mutations of FGFR3 in human bladder and cervix carcinomas. Nat Genet 23: 18-20, 1999.
11. Greulich H and Pollock PM: Targeting mutant fibroblast growth factor receptors in cancer. Trends Mol Med 17: 283-292, 2011.
12. Cancer Genome Atlas Research Network: Comprehensive genomic characterization of squamous cell lung cancers. Nature 489: 519-525, 2012.
13. Singh D, Chan JM, Zoppoli P, Niola F, Sullivan R, Castano A, Liu EM, Reichel J, Porrati P, Pellegatta S, Qiu K, Gao Z, Ceccarelli M, Riccardi R, Brat DJ, Guha A, Aldape K, Golfinos JG, Zagzag D, Mikkelsen T, Finocchiaro G, Lasorella A, Rabadan R and Iavarone A: Transforming fusions of *FGFR* and *TACC* genes in human glioblastoma. Science 337: 1231-1235, 2012.
14. Williams SV, Hurst CD and Knowles MA: Oncogenic FGFR3 gene fusions in bladder cancer. Hum Mol Genet 22: 795-803, 2013.
15. Wu YM, Su F, Kalyana-Sundaram S, Khazanov N, Ateeq B, Cao X, Lonigro RJ, Vats P, Wang R, Lin SF, Cheng AJ, Kunju LP, Siddiqui J, Tomlins SA, Wyngaard P, Sadis S, Roychowdhury S, Hussain MH, Feng FY, Zalupski MM, Talpaz M, Pienta KJ, Rhodes DR, Robinson DR and Chinnaiyan AM: Identification of targetable FGFR gene fusions in diverse cancers. Cancer Discov 3: 636-647, 2013.
16. Majewski IJ, Mittempergher L, Davidson NM, Bosma A, Willems SM, Horlings HM, de Rink I, Greger L, Hooijer GK, Peters D, Nederlof PM, Hofland I, de Jong J, Wesseling J, Kluin RJ, Brugman W, Kerkhoven R, Nieboer F, Roepman P, Broeks A, Muley TR, Jassem J, Niklinski J, van Zandwijk N, Brazma A, Oshlack A, van den Heuvel M and Bernards R: Identification of recurrent *FGFR3* fusion genes in lung cancer through kinome-centred RNA sequencing. J Pathol 230: 270-276, 2013.
17. Liao RG, Jung J, Tchaicha J, Wilkerson MD, Sivachenko A, Beauchamp EM, Liu Q, Pugh TJ, Pedamallu CS, Hayes DN, Gray NS, Getz G, Wong KK, Haddad RI, Meyerson M and Hammerman PS: Inhibitor-sensitive FGFR2 and FGFR3 mutations in lung squamous cell carcinoma. Cancer Res 73: 5195-5205, 2013.
18. Shinmura K, Goto M, Suzuki M, Tao H, Yamada H, Igarashi H, Matsuura S, Maeda M, Konno H, Matsuda T and Sugimura H: Reduced expression of MUTYH with suppressive activity against mutations caused by 8-hydroxyguanine is a novel predictor of a poor prognosis in human gastric cancer. J Pathol 225: 414-423, 2011.
19. Pao W and Girard N: New driver mutations in non-small-cell lung cancer. Lancet Oncol 12: 175-180, 2011.
20. Ulivi P, Romagnoli M, Chiadini E, Casoni GL, Capelli L, Gurioli C, Zoli W, Saragoni L, Dubini A, Tesei A, Amadori D and Poletti V: Assessment of *EGFR* and *K-ras* mutations in fixed and fresh specimens from transesophageal ultrasound-guided fine needle aspiration in non-small cell lung cancer patients. Int J Oncol 41: 147-152, 2012.
21. Mantripragada K and Khurshid H: Targeting genomic alterations in squamous cell lung cancer. Front Oncol 3: 195, 2013.
22. Pros E, Lantuejoul S, Sanchez-Verde L, Castillo SD, Bonastre E, Suarez-Gauthier A, Conde E, Cigudosa JC, Lopez-Rios F, Torres-Lanzas J, Castellví J, Ramon y Cajal S, Brambilla E and Sanchez-Cespedes M: Determining the profiles and parameters for gene amplification testing of growth factor receptors in lung cancer. Int J Cancer 133: 898-907, 2013.
23. Intini D, Baldini L, Fabris S, Lombardi L, Ciceri G, Maiolo AT and Neri A: Analysis of *FGFR3* gene mutations in multiple myeloma patients with t(4;14). Br J Haematol 114: 362-364, 2001.
24. Petitjean A, Mathe E, Kato S, Ishioka C, Tavtigian SV, Hainaut P and Olivier M: Impact of mutant p53 functional properties on *TP53* mutation patterns and tumor phenotype: lessons from recent developments in the IARC TP53 database. Hum Mutat 28: 622-629, 2007.
25. Yeudall WA, Vaughan CA, Miyazaki H, Ramamoorthy M, Choi MY, Chapman CG, Wang H, Black E, Bulysheva AA, Deb SP, Windle B and Deb S: Gain-of-function mutant p53 upregulates CXC chemokines and enhances cell migration. Carcinogenesis 33: 442-451, 2012.
26. Bromberg Y and Rost B: SNAP: predict effect of non-synonymous polymorphisms on function. Nucleic Acids Res 35: 3823-3835, 2007.

Natsume et al. Journal of Translational Medicine 2012, 10:97
http://www.translational-medicine.com/content/10/1/97

JOURNAL OF TRANSLATIONAL MEDICINE

RESEARCH Open Access

The *CRKL* gene encoding an adaptor protein is amplified, overexpressed, and a possible therapeutic target in gastric cancer

Hiroko Natsume[1], Kazuya Shinmura[1], Hong Tao[1], Hisaki Igarashi[1], Masaya Suzuki[1], Kiyoko Nagura[1], Masanori Goto[1], Hidetaka Yamada[1], Matsuyoshi Maeda[2], Hiroyuki Konno[3], Satoki Nakamura[4] and Haruhiko Sugimura[1*]

Abstract

Background: Genomic DNA amplification is a genetic factor involved in cancer, and some oncogenes, such as *ERBB2*, are highly amplified in gastric cancer. We searched for the possible amplification of other genes in gastric cancer.

Methods and Results: A genome-wide single nucleotide polymorphism microarray analysis was performed using three cell lines of differentiated gastric cancers, and 22 genes (including *ERBB2*) in five highly amplified chromosome regions (with a copy number of more than 6) were identified. Particular attention was paid to the *CRKL* gene, the product of which is an adaptor protein containing Src homology 2 and 3 (SH2/SH3) domains. An extremely high *CRKL* copy number was confirmed in the MKN74 gastric cancer cell line using fluorescence *in situ* hybridization (FISH), and a high level of CRKL expression was also observed in the cells. The RNA-interference-mediated knockdown of CRKL in MKN74 disclosed the ability of CRKL to upregulate gastric cell proliferation. An immunohistochemical analysis revealed that CRKL protein was overexpressed in 24.4% (88/360) of the primary gastric cancers that were analyzed. The *CRKL* copy number was also examined in 360 primary gastric cancers using a FISH analysis, and *CRKL* amplification was found to be associated with CRKL overexpression. Finally, we showed that MKN74 cells with *CRKL* amplification were responsive to the dual Src/BCR-ABL kinase inhibitor BMS354825, likely via the inhibition of CRKL phosphorylation, and that the proliferation of MKN74 cells was suppressed by treatment with a CRKL-targeting peptide.

Conclusion: These results suggested that CRKL protein is overexpressed in a subset of gastric cancers and is associated with *CRKL* amplification in gastric cancer. Furthermore, our results suggested that CRKL protein has the ability to regulate gastric cell proliferation and has the potential to serve as a molecular therapy target for gastric cancer.

Keywords: CRKL, Gastric cancer, Cell proliferation, Overexpression, Copy number amplification

Background

Although the overall incidence of gastric cancer is decreasing in many countries, the high incidence of gastric cancer remains a serious health problem, and gastric cancer continues to be the second-leading cause of cancer-related death worldwide [1,2]. Gastric carcinogenesis is a multi-step process in which environmental and genetic factors interact [1–8]. Among the genetic changes observed in cancerous cells, genomic DNA amplification is a well-known alteration that is involved in gastric cancer [4,5,7]. Amplification is often associated with increased expression levels of the genes contained in the amplified loci [5]. Oncogenes in gastric cancer, such as *MYC* (mapped to chromosome 8q24), *KRAS* (12p12), and *ERBB2* (17q12), are located in such amplified regions [4,5,7,9]. We considered the possibility that there exist genes whose amplification in gastric cancer has not been revealed to date. To uncover such novel gene alterations, we searched for highly amplified genes in

* Correspondence: hsugimur@hama-med.ac.jp
[1]Department of Tumor Pathology, Hamamatsu University School of Medicine, 1-20-1 Handayama, Higashi Ward, Hamamatsu, Shizuoka 431-3192, Japan
Full list of author information is available at the end of the article

gastric cancer using a genome-wide single nucleotide polymorphism (SNP) microarray analysis and found that the *CRKL* [*v-crk sarcoma virus CT10 oncogene homolog (avian)-like*] gene (22q11) is highly amplified in gastric cancer. The CRKL, a member of the CRK family of adapter proteins, consists of an NH2-terminal Src homology 2 (SH2) domain followed by two SH3 domains: SH3n and SH3c [10], and participates in signal transduction in response to growth factors, cytokines, and the oncogenic BCR-ABL fusion protein, resulting in cell proliferation, survival, adhesion, and migration [10,11]. We hypothesized that CRKL might play an important role in gastric carcinogenesis and investigated whether CRKL expression and the function of CRKL protein affect the regulation of cell proliferation in gastric cancer. We also investigated responsiveness of a gastric cancer cell line containing *CRKL* amplification to a kinase inhibitor, BMS354825, and a CRKL-targeting peptide.

Materials and Methods

Cell lines and surgical specimens

The gastric adenocarcinoma cell lines MKN7, MKN28, MKN74, and AGS were purchased from the Human Science Research Resource Bank (Osaka, Japan) or from American Type Culture Collection (Manassas, VA). Cells were cultured and grown in RPMI 1640 medium supplemented with 10% fetal bovine serum, penicillin (100 units/mL), and streptomycin (100 μg/mL) under a 5% CO_2 atmosphere at 37°C. Paraffin-embedded gastric tissues obtained from gastric cancer patients who underwent surgery at Toyohashi Municipal Hospital (Japan) were used for the immunohistochemical analysis. Gastric tissue samples obtained from gastric cancer patients who underwent surgery at Hamamatsu University Hospital (Japan) were used for the quantitative reverse-transcription (QRT)-polymerase chain reaction (PCR) analysis. The study design was approved by the Institutional Review Boards (IRBs).

Genome-wide SNP microarray

DNA (250 ng) was digested with *Nsp*I restriction enzyme (New England Biolabs, Hertfordshire, UK) and ligated to a universal adaptor sequence. The ligated DNA was PCR-amplified using primers complementary to the universal adaptors, and the PCR products were purified, quantified, and normalized. The products were then fragmented, end-labeled using terminal deoxynucleotidyl transferase, and hybridized to the Affymetrix GeneChip human mapping 250 K NspI arrays (Affymetrix Japan, Tokyo, Japan). After hybridization, the arrays were washed, stained using Affymetrix fluidics station 450, and scanned with a GeneChip Scanner 3000 7 G. Raw SNP call data were extracted using Affymetrix GeneChip Genotyping Analysis software (GTYPE) 4.1. The SNP microarray data were analyzed to determine the total copy number using the CNAG program, as previously described [12,13] (Figure 1).

WST-8 assay

Cell proliferation and viability were quantified using a Cell Counting Kit-8 (Dojindo, Kumamoto, Japan) according to the manufacturer's instructions [14]. The assay was based on the extracellular reduction of the tetrazolium salt WST-8 by NADH produced in the mitochondria of living cells. The cells were incubated with the WST-8 reagent for 1 hr at 37°C, and the absorbance was measured at 450 nm using an EL340I microplate reader (BIO-TEK Instruments, Winooski, VT) (Figure 2).

Immunohistochemistry

Tissue microarray (TMA) blocks were prepared as previously described [14-16]. TMA block sections were deparaffinized, rehydrated, and boiled in Tris-EDTA buffer (pH 9.0) for antigen retrieval. Endogenous peroxidase activity was blocked by incubation in a hydrogen peroxide solution. Next, the sections were incubated with a rabbit anti-CRKL monoclonal antibody (Y243; Abcam, Cambridge, UK). The antigen-antibody complex was visualized using Histofine Simple Stain Max-Po (Multi) (Nichirei, Tokyo, Japan) and 3,3'-diaminobenzidine tetrahydrochloride. Counterstaining was performed using hematoxylin. The intensity values of the cells were determined using a 4-point scale according to the color of the cell cytoplasm after CRKL immunostaining as follows: 0, blue; 1, blue-brown; 2, light brown; and 3, brown. The percentage of cells with each intensity value was then multiplied by the intensity value, as described previously [14]. The scores obtained for CRKL immunostaining were classified as either a low expression level (0–0.99) or a high expression level (1.00–3.00) (Figure 3).

DNA fluorescence *in situ* hybridization (FISH)

FISH was performed as previously described [16-19]. Tissue slides were hybridized with a Spectrum Orange-labeled BAC clone (RP11-801O20 and RP11-1058B20) for the *CRKL* locus (Advanced GenoTechs Co., Tsukuba, Japan) and a Spectrum Green-labeled control probe for the near centromere locus on chromosome 22 (BAC clone: RP11-232E17). 4',6-Diamidino-2-phenylindole (DAPI) (Vector Laboratories, Burlingame, CA) was used for nuclear staining (Figure 3).

MTT assay and direct cell counting

In the experiment involving treatment with the CRKL-targeting peptide, an MTT assay was performed to assess cell viability in Figure 4G. The cells were cultured with the indicated concentration of CRKL-targeting peptide or dimethyl sulfoxide (DMSO) at 37°C for 72 h, and 3-(4,5-dimethylthiazol-2-yl)-2,5-diphenyltetrazolium